



Analysis of instability patterns in acute scaphoid fractures by 4-dimensional computed tomographic imaging – A prospective cohort pilot study protocol

M.G.A. de Roo^{a,b,*}, J.G.G. Dobbe^b, M.L. Ridderikhof^c, J.C. Goslings^d, C.M.A.M. van der Horst^a, L.F.M. Beenen^e, G.J. Streekstra^{b,e}, S.D. Strackee^a

^a Department of Plastic, Reconstructive and Hand Surgery, Academic Medical Center, University of Amsterdam, Amsterdam Movement Sciences, Amsterdam, The Netherlands

^b Department of Biomedical Engineering and Physics, Academic Medical Center, University of Amsterdam, Amsterdam Movement Sciences, Amsterdam, The Netherlands

^c Department of Emergency Medicine, Academic Medical Center, University of Amsterdam, Amsterdam, The Netherlands

^d Trauma Unit, Department of Surgery, Academic Medical Center, University of Amsterdam, Amsterdam Movement Sciences, Amsterdam, The Netherlands

^e Department of Radiology, Academic Medical Center, University of Amsterdam, Amsterdam Movement Sciences, Amsterdam, The Netherlands

ARTICLE INFO

Article history:

Received 12 January 2018

Received in revised form 16 April 2018

Accepted 18 April 2018

Available online 20 April 2018

ABSTRACT

Introduction: A scaphoid fracture is the most common carpal fracture. When healing of the fracture fails (nonunion), a specific pattern of osteoarthritis occurs, resulting in pain, restricted wrist motion and disability. Scaphoid fracture classification systems recognize fragment displacement as an important cause of nonunion. The fracture is considered unstable if the fragments are displaced. However, whether and how displaced bone fragments move with respect to one another has not yet been investigated in vivo. With a four-dimensional (4D) computed tomographic (CT) imaging technique we aim to analyze the interfragmentary motion patterns of displaced and non-displaced scaphoid fragments. Furthermore, the correlation between fragment motion and the development of a scaphoid nonunion is investigated. We hypothesize that fragment displacement is not correlated to fragment instability; and concurrent nonunion is related to fragment instability and not to interfragmentary displacement.

Methods: In a prospective single-center cohort pilot study, patients with a one-sided acute scaphoid fracture and no history of trauma to the contralateral wrist are eligible for inclusion. Twelve patients with a non-displaced scaphoid fracture and 12 patients with a displaced scaphoid fracture are evaluated. Both wrists are scanned with 4D-CT imaging during active flexion–extension and radio-ulnar deviation motion. The contralateral wrist serves as kinematic reference. Relative displacement of the distal scaphoid fragment with respect to the proximal scaphoid fragment, is described by translations and rotations (the kinematic parameters), as a function of the position of the capitate. Non-displaced scaphoid fractures are treated conservatively, displaced scaphoid fractures receive intraoperative screw fixation. Follow-up with CT scans is conducted until consolidation at 1½, 3 and 6 months. This trial is registered in the Dutch Toetsingonline trial registration system, number: NL60680.018.17.

Ethics: This study is approved by the Medical Ethics Committee of the Academic Medical Center, Amsterdam.

© 2018 The Authors. Published by Elsevier Ltd on behalf of Surgical Associates Ltd. This is an open access article under the CC BY-NC-ND license (<http://creativecommons.org/licenses/by-nc-nd/4.0/>).

1. Introduction

The human wrist is a complex arrangement of eight carpal bones (Fig. 1). Within the collection of carpal bones, the scaphoid plays a key role in carpal stability and wrist mechanics [1]. Scaphoid fractures account for approximately 60–70% of all carpal fractures [2], which predominantly occur in young, active men of working age who fall onto an outstretched hand [3]. When healing of the fracture fails (nonunion), the period in which the hand is immobilized sometimes exceeds 4–6 months, resulting in productivity loss and associated costs for society [4].

Abbreviations: 3D, three-dimensional; 4D, four-dimensional; AMC, academic medical center; CT, computed tomographic; FE, flexion–extension; mm, millimeter; mSv, millisievert; RU, radioulnar.

* Corresponding author at: Department of Plastic, Reconstructive and Hand Surgery, Academic Medical Center, University of Amsterdam, Meibergdreef 9, 1105 AZ Amsterdam, The Netherlands. Fax: +31 020 691 7549.

E-mail address: m.g.deroo@amc.uva.nl (M.G.A. de Roo).

<https://doi.org/10.1016/j.isjp.2018.04.003>

2468-3574/© 2018 The Authors. Published by Elsevier Ltd on behalf of Surgical Associates Ltd.

This is an open access article under the CC BY-NC-ND license (<http://creativecommons.org/licenses/by-nc-nd/4.0/>).

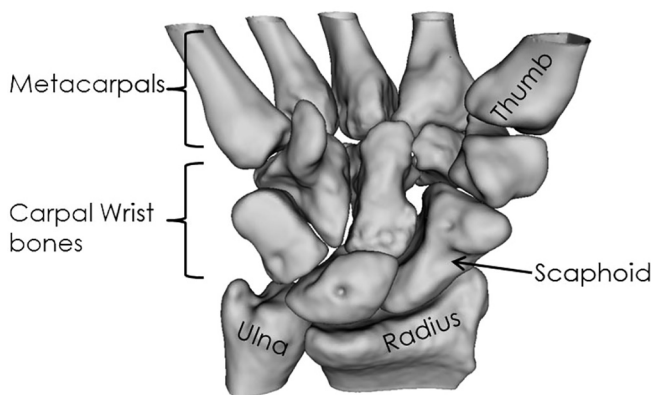


Fig. 1. The scaphoid articulates with 5 surrounding bones. It plays a key role in the stability of the wrist and wrist mechanics.

To identify fractures that are prone to nonunion, 13 different scaphoid fracture classification systems are available. The classification systems are based on (1) fracture location, (2) fracture plane orientation, and (3) fracture stability/dislocation [5]. Although scaphoid fractures have an overall union rate of 90%, scaphoid bone fragments with a 1-mm (mm) dislocation are associated with union rates up to only 55% [6]. Within the group of patients with a dislocation it is not clear why the union rate is low, since fundamental understanding of mechanisms and causes of poor healing are lacking. An important reason for this knowledge gap is that current diagnosis of fragment instability is based on plain radiographs or CT scans of a static wrist. Steady-state imaging cannot reveal inter-fragmentary scaphoid motion when moving the wrist [7], although it is likely that inter-fragmentary motion will play an important role in fracture healing [8]. We hypothesize that fragment displacement is not correlated to fragment instability; and concurrent nonunion is related to inter-fragmentary motion and not to interfragmentary dislocation.

2. Aim of the trial

Primary objective: What are the differences of interfragmentary motion patterns between displaced and non-displaced scaphoid fracture fragments?

Secondary objective: Is there a correlation between the motion patterns found between scaphoid fracture fragments and the development of a scaphoid nonunion?

3. Methods

3.1. Study population

All patients with an acute scaphoid fracture are informed about the research project during their visit to the emergency department. Information is provided through personal explanation and written brochures. Subjects are included after signing a written informed consent.

3.1.1. Inclusion criteria

- Patients with a one-sided acute scaphoid fracture (on radiograph or CT scan)
- Patients are over the age of 16 years
- Patients who are willing and able to give informed consent

3.1.2. Exclusion criteria

- History of trauma (treated with a cast or surgically) to the contralateral non-fractured wrist
- Not able to understand the written informed consent
- (Peri-)lunar dislocation
- Pain, to the degree that the patient is not able or willing to move the hand

3.2. Trial site and sample size calculation

This protocol describes a prospective cohort pilot study and will be conducted at the Academic Medical Center (AMC), Amsterdam. It is the first time that this technique is used for the clinical evaluation of acute scaphoid fractures. A power analysis is performed with the nQuery advisor program. When the sample size is 12, a two-sided 95% Confidence Interval (95%-CI) for a single mean will extend 0.566δ from the observed mean, assuming that the standard deviation is δ and the confidence interval is based on the large sample z statistic [9]. In total we aim to include 24 participants: 12 participants with a displaced scaphoid fracture and 12 participants with a non-displaced scaphoid fracture.

3.3. Planned study conduct

After inclusion in the emergency department, patients will undergo a standard CT scan and a 4D-CT scan of both wrists with the Somatom Force CT scanner (Somatom Force, Siemens Healthineers, the Netherlands).

Based on the standard CT-scan, the patient will be categorized into:

- Nondisplaced or minimally displaced fractures
- Displaced fractures; defined as a >1-mm step-off between the bone segments. This is measured as a translation of a scaphoid fragment relative to the inertial axis of the scaphoid.

When the patient is in pain, pain medication will be provided, according to the pain medication protocol of the emergency department and on discretion of the treating physician. Patients presented to the emergency department in evenings, nights or weekends and willing to participate, will be scanned during the cast change in the first week after presentation (Fig. 2).

3.3.1. Hand motion protocol

Both wrists of the patient are scanned during flexion–extension (FE) and radioulnar (RU) deviation. The patient is scanned in prone position, with the arm extended forward. The wrist is placed in a special positioning device to immobilize the elbow and to fixate the radius. The device has a grip bar and FE and RU motion axes. The RU axis is locked and a low dose 4D-CT is made in 10 s when the patient moves the wrist actively from extension to flexion. A second 4D-CT scan is made after the FE axis is locked and a 10 s active motion from radial to ulnar deviation follows. First the unharmed wrist is scanned. A regular dose static CT scan of the forearms in neutral position is obtained, to evaluate the alignment of the fracture fragments after wrist motion. The neutral position is accomplished by aligning the third metacarpal with the dorsal surface of the forearm.

3.3.2. Image acquisition

The 10 s of 4D-CT data acquisition will result in 32 volume reconstructions. Each volume reconstruction belongs to a certain position of the hand during the dynamic motion. For reconstruc-

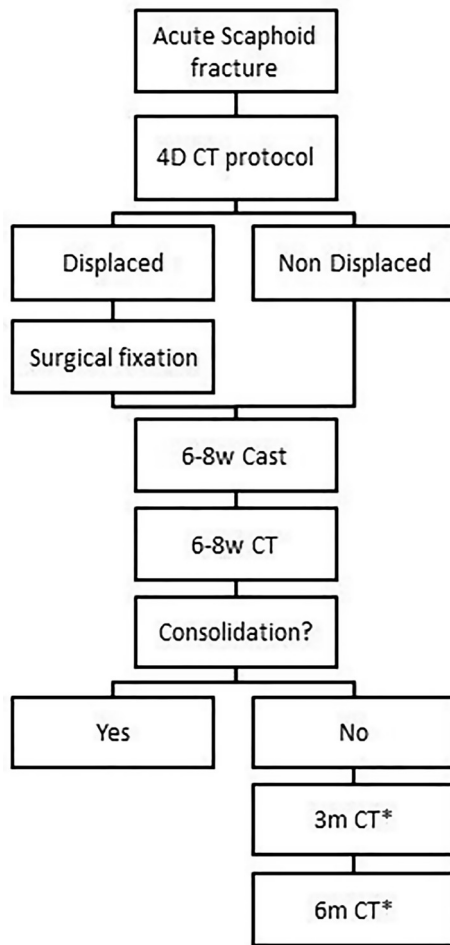


Fig. 2. Workflow diagram for patients with a scaphoid fracture. A 4D-CT scan during flexion-extension and radioulnar deviation of both wrists is obtained. *Patients are followed up until the scaphoid fragments are united.

tion of the bone geometry, we will acquire a regular static 3D-CT scan of the forearm in neutral position, with a slice thickness of 0.6 mm.

3.3.3. Segmentation of carpal bones and radius

The Articul8 program © (Academic Medical Center Amsterdam, University of Amsterdam) is used for segmentation and analysis of the 4D data. Segmentation of the carpal bones and radius is created through threshold-connected region growing, followed by a binary closing algorithm for filling residual holes and closing of the outline based on the regular CT image. Then a Laplacian level-set segmentation growth algorithm is used to advance pixel dispersion toward the edge of the bone [10]. The distal and proximal fragments of the scaphoid are segmented individually. The scans of the left wrists are mirrored to right wrists before segmentation for the purpose of comparing motion patterns.

3.3.4. Registration of translations and rotations of individual bones

After segmentation, the 3D bone models and/or fragments will be registered to the respective frames in the 4D scan. Registration is a semi-automatic procedure, which starts by aligning the bones/segments with the respective bones in the first frame of a 4D scan. If the inter-frame repositioning is relatively small the registration procedure can automatically find the position in consecutive frames [11]. Visual inspection is required to assess whether correct alignment is established.

3.3.5. Identifying the fracture location

The fracture location is quantified by aligning the proximal segment of the affected scaphoid model with the healthy scaphoid model of the contralateral bone. A central axis is determined, along which the healthy scaphoid model is subdivided into three regions of equal length. The regions are used to identify the fracture location. To categorize the fractures, the percentage of the fracture that lies in the proximal, central or distal third part of the scaphoid is determined (Fig. 3). The central axis is further used to quantify the dislocation of the bone segments. The central axis is calculated using the points describing the healthy scaphoid model by calculating the centroid and the moment of inertia tensor. Eigenvector analysis of the inertia tensor provides three eigenvectors and eigenvalues. The central axis runs through the centroid and in the direction of the eigenvector with the smallest eigenvalue.

3.3.6. Describing kinematics

An anatomical coordinate system for the radius will be placed by a computerized positioning algorithm [12]. The origin of the coordinate system is located midway between the radio-scaphoid fossa and the radio-lunate fossa of the distal radius. The Z-axis is parallel to the long shaft of the radius that intersects with the origin. The X-axis is the line perpendicular to the Z-axis in a plane defined by the tip of the radial styloid, the base of the concavity of the sigmoid notch, and the specified origin. The Y-axis is defined as the common line perpendicular to both the X- and Z-axes. The +X-axis is the axis of flexion ($\varphi_x \geq 0^\circ$) and extension ($\varphi_x < 0^\circ$); the +Z-axis is the axis of supination ($\varphi_z \geq 0^\circ$) and pronation ($\varphi_z < 0^\circ$); and the +Y-axis is the axis of radial ($\varphi_y \geq 0^\circ$) and ulnar ($\varphi_y < 0^\circ$) deviation (rotation sequence y,x,z).

3.3.7. Treatment and follow-up

Based on the radiograph or CT scan, used to diagnose the acute scaphoid fracture, the standard treatment care and follow-up will be maintained. Displaced fractures will undergo surgical treatment

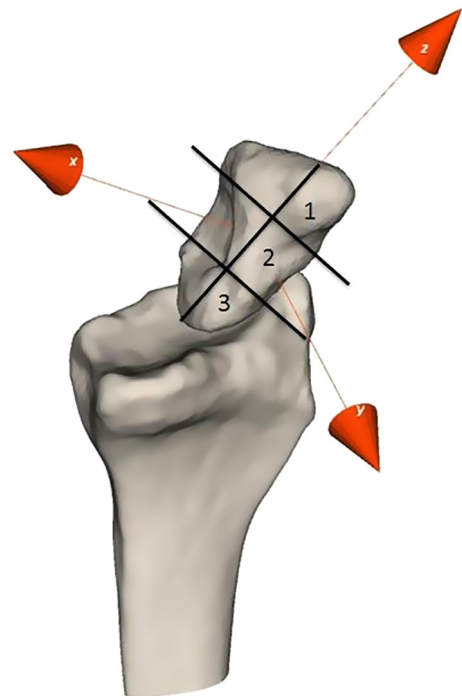


Fig. 3. Division of the scaphoid into three parts of equal length as measured along the central axis: distal (no. 1), central (no. 2) and proximal (no. 3) part of the healthy scaphoid.

by screw fixation; non-displaced fractures will receive cast treatment without immobilization of the thumb [13]. Follow-up will be conducted with CT scans at 1½, 3 and 6 months (Somatom Force, and Somatom AS+, Siemens Healthineers, the Netherlands).

3.4. Statistical analysis

The 4D-CT scan provides 32 different time frames of one motion cycle. We defined global wrist motion as the rotation and translation of the capitate with respect to the radius [14]. The norm of the translation parameters (Δx , Δy , Δz) and rotation parameters (ϕx , ϕy , ϕz) is used to represent the translation and rotation error [15].

To be able to answer what the differences are between interfragmentary motion patterns of displaced and non-displaced scaphoid fracture fragments, the rotation and translation error of the distal scaphoid, relative to the proximal scaphoid during FE and RU motion will be described using a linear mixed model analysis. To correlate the amount of motion to time to union, the Holm test adjusted for multiple comparisons will be used. To evaluate different motion parameters between the injured and non-injured wrist of the same individual, we will use a linear mixed model analysis.

3.5. Methods for minimizing bias

Minimizing selection bias: All patients that meet the inclusion criteria and give informed consent will be included in this trial.

Minimizing attrition bias: The trial is prospectively registered in the Dutch Toetsingonline trial registration system (number: NL60680.018.17). Selective reporting is avoided by publishing this trial protocol according to the STROCSS guideline [16].

Minimizing other bias: Financial relationships and conflicts of interest that could influence the outcomes of the trial will be stated explicitly.

4. Ethics and data protections

This study is approved by the Medical Ethics Committee of the Academic Medical Center, Amsterdam. Publishing the protocol of this study is in compliance with the STROCSS guideline to strengthen reporting in surgical cohort studies [16]. The radiation exposure of 4D-CT scans in addition to conventional CT scanning is within the category IIa (0.1–1 mSv) of the International Commission on Radiological Protection (ICRP), which qualifies as: minor risk. No healthy control group is needed, since the contralateral wrist of the patient is scanned. A subject's identification code list will be used to link the data to the subjects. The investigator will safeguard the key to the code. The handling of personal data complies with the Dutch personal Data Protection Act.

Conflicts of interest

The authors declare that they have no competing interests.

Funding

Financial support for this trial is provided by the AO Foundation – AO Trauma, Switzerland, project no. AOTEURC-2017_011. The AO Foundation was not involved in the design of this study and preparation of this manuscript.

Ethical approval

This study is approved by the Medical Ethics Committee of the Academic Medical Center, Amsterdam. Approval number: 2017_055#B2017237.

Research registration unique identifying number (UIN)

This trial is registered in the Dutch Toetsingonline trial registration system, number: NL60680.018.17 (<https://www.toetsingonline.nl/>).

Author contribution

All authors participated in the design of the study. MGAR: Participated in the design of the study and drafted the manuscript. JGGD: Participated in the design of the study and helped to draft the manuscript. MLR: Participated in the design of the study and helped to draft the manuscript. JCG: Participated in the design of the study and drafted the manuscript. CMAMH: Participated in the design of the study and critical revision of the manuscript. LFMB: Participated in the design of the study and critical revision of the manuscript. GJS: Participated in the design of the study and critical revision of the manuscript. SDS: Participated in the design of the study and critical revision of the manuscript. All authors have read and approved the final study protocol manuscript.

Guarantor

MGA de Roo and SD Strackee are the guarantors of this trial.

Appendix A. Supplementary data

Supplementary data associated with this article can be found, in the online version, at <https://doi.org/10.1016/j.isjp.2018.04.003>.

References

- [1] R.A. Berger, *The anatomy of the scaphoid*, *Hand Clin.* 17 (4) (2001) 525–532.
- [2] S. Alshryda, A. Shah, S. Odak, J. Al-Shryda, B. Ilango, S.R. Murali, Acute fractures of the scaphoid bone: systematic review and meta-analysis, *Surgeon* 10 (4) (2012) 218–229, <https://doi.org/10.1016/j.surge.2012.03.004>.
- [3] V.S. Pao, J. Chang, Scaphoid nonunion: diagnosis and treatment, *Plast. Reconstruct. Surg.* 112 (6) (2003) 1666–1676, <https://doi.org/10.1097/01.PRS.0000086090.43085.66>.
- [4] M.C.E. de Putter, R.W. Selles, S. Polinder, M.J.M. Panneman, S.E.R. Hovius, E.F. van Beeck, Economic impact of hand and wrist injuries: health-care costs and productivity costs in a population-based study, *J. Bone Joint Surg. Am.* (2012), <https://doi.org/10.2106/JBJS.K.00561>.
- [5] P.W. Ten Berg, T. Drijkoningen, S.D. Strackee, G.A. Buijze, Classifications of acute scaphoid fractures: a systematic literature review, *J. Wrist Surg.* 5 (2) (2016) 152–159, <https://doi.org/10.1055/s-0036-1571280>.
- [6] S.J. Rhemrev, D. Ootes, F.J. Beeres, S.A. Meylaerts, I.B. Schipper, Current methods of diagnosis and treatment of scaphoid fractures, *Int. J. Emerg. Med.* 4 (2011) 4, <https://doi.org/10.1186/1865-1380-4-4>.
- [7] E.L. Leventhal, S.W. Wolfe, D.C. Moore, E. Akelman, A.P. Weiss, J.J. Crisco, Interfragmentary motion in patients with scaphoid nonunion, *J. Hand Surg. Am.* 33 (7) (2008) 1108–1115, <https://doi.org/10.1016/j.jhssa.2008.03.008>.
- [8] G.A. Buijze, P. Jorgsholm, N.O. Thomsen, A. Bjorkman, J. Besjakov, D. Ring, Factors associated with arthroscopically determined scaphoid fracture displacement and instability, *J. Hand Surg. Am.* 37 (7) (2012) 1405–1410, <https://doi.org/10.1016/j.jhssa.2012.04.005>.
- [9] S.A. Julious, Sample size of 12 per group rule of thumb for a pilot study, *Pharmaceut. Statist.* 4 (4) (2005) 287–291, <https://doi.org/10.1002/pst.185>.
- [10] J.G. Dobbe, S.D. Strackee, A.W. Schreurs, R. Jonges, B. Carelsen, J.C. Vroemen, C. A. Grimbergen, G.J. Streekstra, Computer-assisted planning and navigation for corrective distal radius osteotomy, based on pre- and intraoperative imaging, *IEEE Trans. Biomed. Eng.* 58 (1) (2011) 182–190, <https://doi.org/10.1109/TBME.2010.2084576>.
- [11] B. Carelsen, R. Jonges, S.D. Strackee, M. Maas, P. van Kemenade, C.A. Grimbergen, M. van Herk, G.J. Streekstra, Detection of in vivo dynamic 3-D

- motion patterns in the wrist joint, *IEEE Trans. Biomed. Eng.* 56 (4) (2009) 1236–1244, <https://doi.org/10.1109/TBME.2008.2009069>.
- [12] J.G. Dobbe, J.C. Vroemen, S.D. Strackee, G.J. Streekstra, Patient-tailored plate for bone fixation and accurate 3D positioning in corrective osteotomy, *Med. Biol. Eng. Comput.* 51 (1–2) (2013) 19–27, <https://doi.org/10.1007/s11517-012-0959-8>.
- [13] G.A. Buijze, J.C. Goslings, S.J. Rhemrev, A.A. Weening, B. Van Dijkman, J.N. Doornberg, D. Ring, Cast immobilization with and without immobilization of the thumb for nondisplaced and minimally displaced scaphoid waist fractures: a multicenter, randomized, controlled trial, *J. Hand Surg. Am.* 39 (4) (2014) 621–627, <https://doi.org/10.1016/j.jhssa.2013.12.039>.
- [14] A. de Lange, J.M. Kauer, R. Huiskes, Kinematic behavior of the human wrist joint: a roentgen-stereophotogrammetric analysis, *J. Orthopaed. Res.* 3 (1) (1985) 56–64, <https://doi.org/10.1002/jor.1100030107>.
- [15] H.-R.S. Hao-Yuan Kuo, Shang-Hong Lai, Wu Chin-Chia, 3D Object Detection and Pose Estimatio from Depth Image for Robotic Bin Picking, in: *IEEE International Conference on Automation Science and Engineering (CASE)*, Taipei, 2014, pp. 1264–1269, <https://doi.org/10.1109/CoASE.2014.6899489>.
- [16] R.A. Agha, M.R. Borrelli, M. Vella-Baldacchino, R. Thavayogan, D.P. Orgill, S. Group, The STROCSS statement: strengthening the reporting of cohort studies in surgery, *Int. J. Surg.* 46 (2017) 198–202, <https://doi.org/10.1016/j.ijssu.2017.08.586>.